Article

The Synchronisation Problem of Chaotic Neural Networks Based on Saturation Impulsive Control and Intermittent Control

Zhengran Cao [1], Chuandong Li [1] and Man-Fai Leung [2,*]

1   Chongqing Key Laboratory of Nonlinear Circuits and Intelligent Information Processing, School of Electronic and Information, Southwest University, Chongqing 400715 , China; zhrcao_swu@163.com (Z.C.); cdli@swu.edu.cn (C.L.)
2   School of Computing and Information Science, Faculty of Science and Engineering, Anglia Ruskin University, Cambridge CB1 1PT, UK
*   Correspondence: man-fai.leung@aru.ac.uk

Abstract: This paper primarily focuses on the chaos synchronisation analysis of neural networks (NNs) under a hybrid controller. Firstly, we design a suitable hybrid controller with saturated impulse control, combined with time-dependent intermittent control. Both controls are low-energy consumption and discrete, aligning well with industrial development needs. Secondly, the saturation function in the chaotic neural network is addressed using the polyhedral representation method and the sector nonlinearity method, respectively. By integrating the Lyapunov stability theory, Jensen's inequality, the mathematical induction method, and the inequality reduction technique, we establish suitable time-dependent Lyapunov generalised equations. This leads to the estimation of the domain of attraction and the derivation of local exponential stability conditions for the error system. The validity of the achieved theoretical criteria is eventually demonstrated through numerical experiment simulations.

Keywords: chaos synchronisation; neural networks; actuator saturation; hybrid controller; Lyapunov Stability Control

MSC: 93C27

1. Introduction

In current scientific research, chaotic neural networks hold significant importance, notably within the burgeoning field of artificial intelligence and its associated methodologies [1–3]. This includes nonlinear modelling and exploration of complex systems, information processing and pattern recognition, analysis and control of dynamic behavior, expansion of neural network learning theory, and artificial intelligence [4–8]. The importance of chaotic neural networks for research is not limited to the field of neural networks, but also includes a variety of fields such as complex systems science, information processing, dynamics and behavior analysis, and computational science. Therefore, the study of nonlinear modelling and dynamical behavior of chaotic neural networks is an important part of the foundation for the development of chaotic neural networks.

It must be mentioned that the synchronisation problem is unavoidable when studying the dynamic behavior of chaotic neural networks (CNNs). The analysis of synchronisation of nonlinear systems is an important direction that has received much attention in the current research field and academic discipline. In many cross-cutting research areas such as biological neural networks [9], learning systems [10], and data processing [11]. The study of synchronous phenomena not only contributes to a deeper understanding of the intrinsic dynamical behaviour of the system, but also provides potential opportunities for practical applications. As the name implies, synchronisation of a class of NNs under a certain network topology focuses on the dynamic behaviour of a group of neural nodes that can

gradually achieve synchronisation in the presence of an information interaction or in the presence of a controller steering. Due to the wide range of industrial applications of neural network synchronisation, many academic results on synchronisation of NNs have emerged in the past decade [12–15].

In the study of synchronisation problems in neural networks, the question of how to achieve fast synchronisation and how to use less energy to do has become a hot topic for researchers. Researchers and scholars have tried to solve the synchronisation problem of neural networks using various control methods: Sliding mode control, impulse control, intermittent control, etc. Among the many control methods, impulse control is generally regarded as a simple, classical and highly manoeuvrable control method for synchronisation due to its uniqueness and ease of implementation. In recent years, many meaningful research results have also been obtained on the design of impulse control protocols or impulse control gains for synchronisation of neural networks [16–20].

On the other hand, intermittent control has gained considerable importance over the last decade, as it has the potential to solve complex control problems that cannot be adequately tackled by traditional continuous control strategies. The significance of intermittent control research lies in its ability to more effectively manage systems with uncertainties, constraints, disturbances, and nonlinear dynamics. Intermittent control is used in various industrial applications such as robotics, energy systems, biological systems, network systems and transportation, and has produced a number of significant research results [21–25]. Wu [21] studied the problem of fixed-time synchronisation of nonlinear systems via intermittent control. Zhong [22] focused on the hybrid mechanism for networked control systems. However, very little research has been conducted on hybrid controllers. Utilizing the advantages of impulsive and intermittent control for hybrid control of nonlinear systems is more useful in engineering applications.

Finally, any physical actuator can be saturated with an upper power limit, due to hardware problems. If the actuator saturation phenomenon is ignored when designing a closed-loop industrial system controller, the performance of the controlled system will decrease when the controller reaches saturation, and in extreme cases, the controlled system may become unstable. Therefore, the phenomenon of actuator saturation is a factor that should not be ignored when studying closed-loop control systems. Many interesting results have also been obtained on actuator saturation [26–30]. Hu [26] takes full account of the saturation phenomenon characteristics and uses the convex combination technique to represent the saturation control as a series of convex packet forms. Li combined impulse control with actuator saturation to obtain a number of columns of results on saturated impulse control [31–34]. Two methods for solving the impulse saturation problem are proposed: the dead-zone nonlinear method and the polyhedral representation. Besides, many scholars have also applied impulse saturation control theory to multi-intelligent body systems, complex networks, and other related fields [35–38].

Based on the above, this paper fully considers the effect of actuator saturation on CNNs and designs a hybrid controller containing impulse control and intermittent control to study the synchronisation problem of CNNs. The main innovations are

- A hybrid controller containing impulse control and intermittent control is designed.
- The effect of saturation on the controller is fully considered, and the saturation function is processed by two methods to obtain a synchronisation criterion that reflects the saturation characteristics.
- Using the linear matrix inequality (LMI) and some effective lemmas, a much less conservative synchronisation criterion is obtained.

The main structure of the paper is: Section 2 gives a series of lemmas, assumptions, and definitions; moreover, it establishes an accurate mathematical model and proposes the controller. Section 3 gives the process of theoretical proof and presents two theorems. Section 4 verifies the obtained theoretical results with experimental simulations. Section 5 gives the conclusion.

2. Preliminary and Mathematical Modelling

We give the necessary lemmas, assumptions and definitions to support the theoretical proof of the paper in this section.

2.1. Lemmas

Some Lemmas are given as follows.

Lemma 1 ([39]). *Let $m \geqslant 1$ be a given integer value, u, $v \in \mathbb{R}^m$ denote two given vectors. If $\|v\|_\infty \leqslant 1$ holds. Then, for $\forall u \in \mathbb{R}^m$, the following equation holds.*

$$\text{Sat}(u) \in \text{co}\{\mathscr{D}_\iota u + \mathscr{D}_\iota^- v : \iota \in \mathbb{I}[1,\ 2^m]\}, \tag{1}$$

where, co denotes the convex hull after the transformation of the saturation function, $\mathscr{D}_\jmath \in \mathscr{D}$, $\mathscr{D}_\jmath^- = I - \mathscr{D}_\jmath$, $\mathbb{I}[1,\ 2^m]$ denotes $\{1, 2, 3, ..., 2^m\}$.

Lemma 2 ((Jensen's Inequality) [40,41]). *There exist arbitrary constant matrices $\mathfrak{J} = \mathfrak{J}^T > 0 \in \mathbb{R}^{n \times n}$, and productable function $g(s)$, $s \in [a,\ b]$ such that the inequality (2) holds:*

$$(b-a) \int_a^b g^T(s) \mathfrak{J} g(s) ds \geq \left(\int_a^b g(s) ds\right)^T \mathfrak{J} \left(\int_a^b g(s) ds\right). \tag{2}$$

Lemma 3 ((Wirtinger Correlation Inequality) [42]). *There exists a symmetric matrix $\mathfrak{G}$ and an arbitrary differentiable function $v(s)$, $s \in [a, b]$, such that the following inequalities hold:*

$$
\begin{aligned}
(b-a) \int_a^b \dot{v}^T(s) \mathfrak{G} \dot{v}(s) ds &\geq \Sigma_1^T \begin{bmatrix} 4\mathfrak{G} & 2\mathfrak{G} & -6\mathfrak{G} \\ * & 4\mathfrak{G} & -6\mathfrak{G} \\ * & * & 12\mathfrak{G} \end{bmatrix} \Sigma_1, \\
\int_a^b \int_v^b \dot{v}^T(s) \mathfrak{G} \dot{v}(s) ds dv &\geq \Sigma_2^T \begin{bmatrix} 2\mathfrak{G} & -2\mathfrak{G} \\ * & 2\mathfrak{G} \end{bmatrix} \Sigma_2,
\end{aligned}
\tag{3}
$$

where $\Sigma_1 = \text{col}\{v(b),\ v(a),\ \frac{1}{b-a} \int_a^b v(s) ds\}$ and $\Sigma_2 = \text{col}\{v(b),\ \frac{1}{b-a} \int_a^b v(s) ds\}$.

Lemma 4 ((Schur Complement Lemma) [42]). *There exist three constant matrices $\mathfrak{Z}_1 = \mathfrak{Z}_1^T < 0$, $\mathfrak{Z}_2 = \mathfrak{Z}_2^T < 0$, $\mathfrak{Z}_3$, $\mathfrak{Z}_1 - \mathfrak{Z}_3^T \mathfrak{Z}_2^{-1} \mathfrak{Z}_3 < 0$ holds if and only if the following inequality exists.*

$$\begin{bmatrix} \mathfrak{Z}_1 & \mathfrak{Z}_3^T \\ * & \mathfrak{Z}_2 \end{bmatrix} < 0, \quad \begin{bmatrix} \mathfrak{Z}_2 & \mathfrak{Z}_3 \\ * & \mathfrak{Z}_1 \end{bmatrix} < 0.$$

Lemma 5 ((Generalised Sector Condition) [43]). *There exist two vectors $\gamma = [\gamma_1, \gamma_2, ..., \gamma_n]^T \in \mathbb{R}^n$ and $\mu = [\mu_1, \mu_2, ..., \mu_n]^T \in \mathbb{R}^n$ satisfying the following condition $|\mu_i - \gamma_i| \leqslant \bar{\mu}_0$, $\bar{\mu}_0 > 0$. The following inequality holds for any diagonal matrix $P \in \mathbb{R}^{n \times n}$.*

$$\kappa(\mu) P[\kappa(\mu) - \gamma] \leqslant 0,$$

where $\kappa(\mu)$ denote the nonlinear function.

2.2. Assumptions and Definitions

Assumption 1. *There exists a nonlinear activation function $f_i(\cdot) : \mathbb{R} \to \mathbb{R}$ satisfying the Lipschitz condition. In other words, there exists a constant $\hat{\alpha}_i > 0$ such that $\forall z_1,\ z_2 \in \mathbb{R}$, one have*

$$0 \leqslant \frac{f_i(z_1) - f_i(z_2)}{z_1 - z_2} \leqslant \hat{\alpha}_i \tag{4}$$

Assumption 2. *Let T_M, T_m be the constants, which $T_M \geqslant T_m > 0$ such that the impulse time sequence $\{t_k\} \in \mathcal{S}(T_m, T_M)$, where $\mathcal{S}(T_m, T_M)$ denotes a class of time series $\{t_k\}$ and satisfies $0 \leqslant t_{k+1} - t_k = T_K \in [T_m, T_M], k \in \mathbb{N}$.*

Assumption 3. *Given the constant $\mathcal{T}_k$, it is guaranteed that $\mathcal{T}_k$ exists in the impulsive interval (t_k, t_{k+1}) and has $0 < \mathcal{T}_k < t_{k+1} - t_k < \infty$.*

Definition 1. *Let κ and τ be positive constants. And if every solution of $v(t)$ in the error system is satisfied*

$$\|v(t)\| \leqslant \kappa e^{-\tau(t-t_0)} \|v(t_0)\|, \forall t \geqslant t_0.$$

Then, the error system is said to be exponentially stable.

Definition 2. *The region R_A denotes the domain of attraction of the error system about the origin, where*

$$R_A = \left\{ v \in \mathbb{R}^n : \lim_{t \to \infty} v(t, v(t_0)) = 0 \right\}.$$

2.3. Model Description

In the paper, the following NNs are considered

$$\dot{\xi}(t) = -D\xi(t) + EF(\xi(t)) + I(t), \tag{5}$$

where, $\xi(t) = \{\xi_1(t), \xi_2(t), ..., \xi_n(t)\}^T \in \mathbb{R}^n$ denotes the state variable of the ith neuron node at time point t. $D \in \mathbb{R}^{n \times n}$ and $E \in \mathbb{R}^{n \times n}$ are denoted as connection weighting coefficient matrices. $F(\xi) \in \mathbb{R}^n$ denotes the activation function of each neuron node. $I(t) = [I_1(t), I_2(t), ..., I_n(t)]^T \in \mathbb{R}^n$ is external inputs to the system.

Moreover, in order to explore the synchronisation problem of NNs with intermittent impulse control for the drive system (5), the following response system with intermittent and saturation impulse controllers is designed in this section.

$$\dot{\omega}(t) = -D\omega(t) + EF(\omega(t)) + \mathbb{U} + I(t), \tag{6}$$

where $\mathbb{U}$ denotes the designed intermittent saturation impulse controllers. The $\omega(t)$ denotes the state variable of the corresponding system. In addition, the matrices D, E, the activation function $F(\omega(t))$, and the external input $I(t)$ satisfy the form described in the system (5), respectively.

The primary objective of the paper is to propose an appropriate hybrid control strategy consisting of saturation impulsive control and intermittent control to propel the system (6) with the system (5) to be synchronised.

Based on the above considerations, the following hybrid controller is designed in this paper

$$\mathbb{U} = \hat{U}(t) + U(t_k), \tag{7}$$

for which

$$\hat{U}(t) = -\exp\{-\alpha(t - t_k)\}\hat{\mathcal{W}}(t)(\xi(t) - \omega(t)), \tag{8}$$

And, the $\hat{U}(t)$ denotes the term of intermittent control of the proposed hybrid controller from paper [23]. Moreover, there are

$$\hat{\mathcal{W}}(t) = \begin{cases} \mathcal{W}, & t_k \leqslant t < t_k + \mathcal{T}_k, \ k \in \mathbb{R}_0 \\ 0, & t_k + \mathcal{T}_k \leqslant t < t_{k+1}, \end{cases} \tag{9}$$

and the term of the saturation impulsive control in the hybrid controller is defined as follows

$$U(t_k) = \text{Sat}\{u(t_k^-)\}\delta(t - t_k), \tag{10}$$

where α is the given scalar and $\hat{\mathscr{W}}(t)$ is the control gain vector, where $\mathscr{W} \in \mathbb{R}^+$. $\{t_k\}$ denotes the sampling time sequences and satisfies the following: $0 \leq t_0 < t_1 < \cdots < t_k < \cdots$, $\lim_{t \to +\infty} t_k = +\infty$. $\delta(\cdot)$ denotes the Dirac function.

$\mathscr{T}_k$ satisfies Assumption 3. In addition, there exist constants $T > \theta > 0$ such that $inf_{k \in N}\{\mathscr{T}_k + t_k - t_k\} = \theta$ and $sup_{k \in N}\{t_{k+1} - t_k\} = T$. Let $L = \frac{\theta}{T}$, it is obvious to conclude that $L \in (0, 1)$. It is worth mentioning that ε denotes the minimum proportion of intermittent control work width $\mathscr{T}_k$ in the time interval $t_{k+1} - t_k$ for all $k \in N$.

Suppose that $\text{Sat}\{u(t)\} = [\text{Sat}\{u_1(t)\}, \cdots, \text{Sat}\{u_n(t)\}]^T \colon \mathbb{R}^n \to \mathbb{R}^n$ is the Standard Vector-valued Saturation Function (SVSF) with saturation level $\bar{u}_0 > 0$.

$$\text{Sat}\{u_i(t)\} = \text{sign}((u_i(t)) \min\{\bar{u}_0, |u_i(t)|\}$$

where $\bar{u}_0$ denotes the saturation level of the saturation function, $u_i(t) = K\{\xi_i(t) - \omega_i(t)\}$, $K \in \mathbb{R}^{n \times n}$ is the gain constants matrix of saturate impulsive.

Remark 1. *The monitoring and measurement of the system state is performed at fixed sampling points, and the instant of impulse occurrence is also performed at the above sampling points in the hybrid controller (7). The presence of a state-dependent exponential variable $\exp\{-\alpha(t - t_k)\}$ in the intermittent control allows the controller to be better controlled according to the state of time, and only in the $[t_k, t_k + \mathscr{T}_k)$ region the intermittent controller is activated.*

Remark 2. *The part of intermittent control (8) can be converted to periodic intermittent control*

$$\hat{U}_i(t) = \begin{cases} \hat{U}_i(t), \ t_0 + k\tau \leqslant t \leqslant t_0 + (k + \alpha)\tau, \\[2mm] 0, \ t_0 + (k + \alpha)\tau < t < t_0 + (k + 1)\tau. \end{cases} \tag{11}$$

Obviously, the above intermittent control protocol (8) is a classical frame protocol that can represent both periodic and non-periodic forms.

Remark 3. *In response systems, a class of hybrid controllers consisting of two control strategies is considered. Where the intermittent controller incorporates the $\exp\{-\alpha(t - t_k)\}$ term, it can be seen that the gap control is related to the current time state and the impulsive instant, which can also be reflected in the saturated impulse intermittent controller designed in this paper when the control amplitude is continuously adjusted based on the feedback from the pulse state and the intermittent control state.*

3. Main Results

Some sufficient criteria for the error system to converge to the origin are given using linear matrix inequalities, Lyapunov–Krasovskii generalised methods and inequality techniques in the section. Two main approaches to deal with the saturation term are utilised: the first is the sector nonlinear modeling approach, which uses the dead zone nonlinearity instead of the saturation term, and the second is the polyhedral representation approach, which represents the saturation function as a convex package.

3.1. Synchronisation Analysis Based on PRs

Based on Lemma 1, it exist a matrix $H \in \mathbb{R}^{n \times n}$ such that $\omega(t_k^-) \in \mathfrak{N} = \{\omega \in \mathbb{R}^n : |H_{(i)}\omega| \leqslant \bar{u}_0\}, \forall i \in [1, n]$. Then, one can claimed that $\text{Sat}\{\mathscr{V}\omega(t_k^-)\} \in \text{co}\{\mathscr{D}_J K\omega(t_k^-) + \mathscr{D}_J^- H\omega(t_k^-)\}$. Therefore, it can be obtained

$$\text{Sat}\{K\omega(t_k^-)\} = \sum_{J=1}^{2^n} \varsigma_J \left(\mathscr{D}_J K + \mathscr{D}_J^- H\right)\omega(t_k^-) \tag{12}$$

for which $\sum_{j=1}^{2^n} \varsigma_j = 1$, $0 \leqslant \lambda_j(t_k^-)$, $k \in \mathbb{N}$, $j \in [1, 2^n]$. $\nu_i(t, x) = \xi_i(t) - \omega_i(t)$, $\epsilon > 0$ is the error state variable of the driver system (5) and the response system (6). According to the (7), we can definite the hybrid controller $\mathbb{U}_i$. Substituting $\mathbb{U}_i$ into (6) yields that

$$
\begin{cases}
\dot{\nu}(t) = -D\nu(t) + E\hat{F}(\nu_i(t)) + \exp\{-\alpha(t - t_k)\}\mathscr{W}\nu(t_k), & t \in [t_k, t_k + \mathscr{T}_k), \\
\dot{\nu}(t) = -D\nu(t) + E\hat{F}(\nu_i(t)), & t \in [t_k + \mathscr{T}_k, t_{k+1}), \\
\Delta\nu(t_{k+1}) = \sum_{j=1}^{2^n} \varsigma_j \left(\mathscr{D}_j K + \mathscr{D}_j^- H\right)\nu\left(t_{k+1}^-\right), & t = t_{k+1},
\end{cases}
\tag{13}
$$

where $\nu(t) = [\nu_1(t), \nu_2(t), \cdots, \nu_n(t)]^T$, $\hat{F}(\nu(t)) = F(\xi(t)) - F(\omega(t))$, $\Delta\nu(t_{k+1}) = \nu(t_{k+1}^+) - \nu(t_{k+1}^-)$, $\nu(t_k) = \nu(t_k^+) = \lim_{t \to t_k^+} \nu(t, x)$, $\nu(t_k^-) = \lim_{t \to t_k^-} \nu(t)$.

Let $e(t) = \exp\{\alpha t\}\nu(t)$. Then the error system converts into

$$
\begin{cases}
\dot{e}(t) = (\alpha I - D)e(t) + E\hat{F}(e_i(t)) + \mathscr{W}e(t_k), & t \in [t_k, t_k + \mathscr{T}_k), \\
\dot{e}(t) = (\alpha I - D)e(t) + E\hat{F}(e_i(t)), & t \in [t_k + \mathscr{T}_k, t_{k+1}), \\
\Delta e(t_{k+1}) = \sum_{j=1}^{2^n} \varsigma_j \left(\mathscr{D}_j K + \mathscr{D}_j^- H\right)e\left(t_{k+1}^-\right), & t = t_{k+1}.
\end{cases}
\tag{14}
$$

Remark 4. *The whole error system* (14) *can be described as three parts: an intermittent control part in the interval* $[t_k, t_k + \mathscr{T}_k)$*, a non-additive controller part in the interval* $[t_k + \mathscr{T}_k, t_{k+1})$ *and a saturated impulse control part in the time instants* $t = t_{k+1}$*.*

Theorem 1. *For given constants* $T_M > T_m \geqslant 0$*,* $\varpi > 0$*,* $\pi > 0$*,* $\alpha > 0$*,* $\epsilon \leqslant 0$*,* $\varsigma_j \in [0, 1]$ *and* $\sum_{j=1}^{2^n} \varsigma_j = 1$ *and given matrices* $H, K, \mathscr{W}, D \in \mathbb{R}^{n \times n}$*. Suppose that exist diagonal matrices* $P \in \mathbb{R}^{n \times n}$*, matrices* $\mathcal{G} > 0$*,* $n \times n$ *matrices* $\mathcal{H}_1, \mathcal{H}_2, \eta_1, \eta_2, \mathscr{A}_i, i = 1, ..., 6$*. Then, the LMIs hold for any initial value condition* $\nu(t_0) \in \mathcal{E}\{\mathcal{G}, \varpi\}$*,* $T_k \in \{T_m, T_M\}$*,* $j \in \mathbb{I}[1, n]$*,* $j \in \mathbb{I}[1, 2^n]$*.*

$$
\mathcal{Q} = \begin{bmatrix} \mathcal{Q}_{11} & \mathcal{Q}_{12} \\ * & \mathcal{Q}_{22} \end{bmatrix} \geq 0,
\tag{15}
$$

$$
\mathscr{Z}_1(T_k) = \begin{bmatrix}
\Pi_{11} & \Pi_{12} & \Pi_{13} & \Pi_{14} & \Pi_{15} \\
\star & \Pi_{22} & \Pi_{23} & \Pi_{24} & \Pi_{25} \\
\star & \star & \Pi_{33} & \Pi_{34} & \Pi_{35} \\
\star & \star & \star & \Pi_{44} & \Pi_{45} \\
\star & \star & \star & \star & \Pi_{55}
\end{bmatrix} < 0,
\tag{16}
$$

$$
\mathscr{Z}_2(T_k) = \begin{bmatrix}
\Gamma_{11} & \Gamma_{12} & \Gamma_{13} & \Gamma_{14} & \Gamma_{15} \\
\star & \Gamma_{22} & \Gamma_{23} & \Gamma_{24} & \Gamma_{25} \\
\star & \star & \Gamma_{33} & \Gamma_{34} & \Gamma_{35} \\
\star & \star & \star & \Gamma_{44} & \Gamma_{45} \\
\star & \star & \star & \star & \Gamma_{55}
\end{bmatrix} < 0,
\tag{17}
$$

(1) *If* $\alpha > -\epsilon$*,* $0 < \pi < \exp\{2(\epsilon + \alpha)\}T_m$*, LMIs* (15)–(17) *hold.*

$$
\begin{bmatrix}
\mathcal{G} & H_{(j)}^T \\
\star & \varpi \bar{u}_0^2 \exp\{-2(\epsilon + \alpha)T_m\}
\end{bmatrix} \geq 0,
\tag{18}
$$

$$
\begin{bmatrix}
-\pi \mathcal{G} & \sum_{j=1}^{2^n} \varsigma_j \left(I + \mathscr{D}_j K + \mathscr{D}_j^- H\right)^T \mathcal{G} \\
\star & -\mathcal{G}
\end{bmatrix} \leq 0,
\tag{19}
$$

Then the system (14) *achieves stability at an exponential decay rate* $-\frac{\ln \pi}{2T_M} + \epsilon + \alpha$*.*

(2) *If $0 < \alpha < -\epsilon, 0 < \pi < \exp\{2(\epsilon + \alpha)\}T_m$, linear matrix inequality (15)–(17), (19) and the following LMIs hold. Then the system (14) achieves stability at an exponential decay rate $-\frac{\ln \pi}{2T_M} + \epsilon + \alpha$.*

$$
\begin{bmatrix}
\mathcal{G} & H_{(j)}^T \\
\star & \omega \bar{u}_0^2 \exp\{-2(\epsilon + \alpha)T_m\}
\end{bmatrix} \geq 0,
\tag{20}
$$

(3) *If $\alpha + \epsilon = 0$, there exists a sufficiently small constant $\beta \in (0, -\epsilon)$ so that $0 < \pi < \exp\{2(\epsilon + \alpha)T_m\}$ holds.*

Then, the system (14) achieves stability with an exponential decay rate $(-\frac{\ln \pi}{2T_M}, -\frac{\ln \pi}{2T_M} + \epsilon)$.

In other words, for all initial values in the ellipsoid $\mathcal{E}\{\mathcal{G}, \omega\}$, the response system (6) is locally exponentially synchronised with the driving system (5) under the hybrid controller. In addition, the estimated domain of attraction is $R_A = \mathcal{E}\{\mathcal{G}, \omega\}$.

$$
\mathcal{Q}_{11} = \mathcal{G} + T_M \mathrm{sym}\{\eta_1\} + \mathcal{H}_1, \ \mathcal{Q}_{12} = -T_M \eta_1 - T_M \eta_2 - \mathcal{H}_1,
$$

$$
\mathcal{Q}_{22} = T_M \mathrm{sym}\{\eta_1\} + \mathcal{H}_1,
$$

$$
\Pi_{11} = 4\epsilon\mathcal{G} - 2\mathrm{sym}(\eta_1) - \frac{8}{T_M}\mathfrak{G}_1 - 4\mathfrak{G}_2 + 2\mathscr{A}_1(\alpha I - D) + 2\mathscr{A}_4(\alpha I - D),
$$

$$
\Pi_{12} = 2\eta_1 + 2\eta_2 - \frac{4}{T_M}\mathfrak{G}_1 + 2(\alpha I - D)^T\mathscr{A}_3^T + 2(\alpha I - D)^T\mathscr{A}_6^T + 2\mathscr{A}_1\mathscr{W},
$$

$$
\Pi_{13} = 2\mathscr{A}_1 E + 2\mathscr{A}_4 E + 2\hat{\Phi}P, \ \Pi_{14} = \frac{12}{T_M}\mathfrak{G}_1 + \frac{4}{T_M}\mathfrak{G}_2,
$$

$$
\Pi_{15} = 4\mathcal{G} - 2\mathscr{A}_1 - 2\mathscr{A}_4, \ \Pi_{22} = -\frac{8}{T_M}\mathfrak{G}_1 - 2\mathrm{sym}(\eta_2) + 2\mathscr{A}_3\mathscr{W},
$$

$$
\Pi_{23} = 2\mathscr{A}_3 E + 2\mathscr{A}_6 E, \ \Pi_{24} = \frac{12}{T_M}\mathfrak{G}_1, \ \Pi_{25} = -2\mathscr{A}_4 - 2\mathscr{A}_6, \ \Pi_{33} = -2P, \ \Pi_{34} = 0,
$$

$$
\Pi_{35} = 2E\mathscr{A}_2^T + 2E\mathscr{A}_5^T, \ \Pi_{44} = -\frac{24}{T_M}\mathfrak{G}_1 - 4\mathfrak{G}_2, \ \Pi_{45} = 0,
$$

$$
\Pi_{55} = \frac{T_M T_k}{2}\mathcal{H}_2 - 2\mathscr{A}_2 - 2\mathscr{A}_6, \ \Gamma_{11} = \Pi_{11} + 4\epsilon T_k\left[\mathrm{sym}(\eta_1) + \frac{4}{T_M}\mathfrak{G}_1 + 2\mathfrak{G}_2\right],
$$

$$
\Gamma_{12} = \Pi_{12} + 4\epsilon T_k\left[\frac{2}{T_M}\mathfrak{G}_1 - \eta_1 - \eta_2\right], \ \Gamma_{13} = \Pi_{13},
$$

$$
\Gamma_{14} = \Pi_{14} + 4\epsilon T_k\left[\frac{6}{T_M}\mathfrak{G}_1 - 2\mathfrak{G}_2\right],
$$

$$
\Gamma_{15} = \Pi_{15} + 4\epsilon T_k \mathrm{sym}(\eta_1), \ \Gamma_{22} = \Pi_{22} + 4\epsilon T_k\left[\mathrm{sym}(\eta_2) + \frac{4}{T_M}\mathfrak{G}_1\right],
$$

$$
\Gamma_{23} = \Pi_{23}, \ \Gamma_{24} = \Pi_{24} + 4\epsilon T_k\left[-\frac{6}{T_M}\mathfrak{G}_1\right],
$$

$$
\Gamma_{25} = \Pi_{25} - 4T_k[\eta_1 + \eta_2]^T, \ \Gamma_{33} = \Pi_{33}, \ \Gamma_{34} = 0,
$$

$$
\Gamma_{35} = \Pi_{35}, \ \Gamma_{44} = \Pi_{44} + 4\epsilon T_k\left[\frac{12}{T_M}\mathfrak{G}_1 + 2\mathfrak{G}_2\right], \ \Gamma_{45} = 0,
$$

$$
\Gamma_{55} = \Gamma_{55} + \epsilon T_k(2\mathcal{H}_1 + \frac{T_M}{2}).
$$

Proof of Theorem 1. Consider the Lyapunov–Krasovskii functional consisting of three part as follow

$$
V(t) = V_1(t) + V_2(t) + V_{\mathcal{X}},
\tag{21}
$$

where,

$$
V_1(t) = e^T(t)\mathcal{G}e(t),
\tag{22}
$$

$$
V_2(t) = T_2(t)\int_{t_k}^t \dot{e}^T(s)\mathcal{H}_1\dot{e}(s)ds + T_2(t)\int_{t_k}^t\int_\tau^t \dot{e}^T(s)\mathcal{H}_2\dot{e}(s)dsd\tau,
\tag{23}
$$

$$V_{\mathcal{X}}(t) = T_2(t)\chi_1^T(t)\mathcal{B}\chi_1(t), \tag{24}$$

for which $T_1(t) = t - t_k$, $T_2(t) = t_{k+1} - t$, $\chi_1 = \mathrm{col} e(t)$, $e(t_k)$ and

$$\mathcal{B} = \begin{bmatrix} \eta_1 + \eta_1^T & -\eta_1 - \eta_2 \\ * & \eta_2 + \eta_2^T \end{bmatrix}.$$

Firstly, when $t \in [t_k, t_{k+1})$, based on Lemma 2 and condition (15), it can be shown that $V(t) > 0$ holds. When $T_1 + T_2 \leqslant T_M$ there are

$$
\begin{aligned}
V(t) \geqslant & e^T(t)\mathcal{G}e(t) + T_2(t)\chi_1^T(t)\mathcal{B}\chi_1(t) + T_2 \int_{t_k}^t \dot{e}^T(s)\mathcal{H}_1\dot{e}(s)ds \\
\geqslant & \frac{T_1}{T_M}e^T(t)\mathcal{G}e(t) + \frac{T_2}{T_M}e^T(t)\mathcal{G}e(t) + T_2(t)\chi_1^T(t)\mathcal{B}\chi_1(t). \\
& + \frac{T_2}{T_M}\int_{t_k}^t \dot{e}^T(s)ds\,\mathcal{H}_1\int_{t_k}^t \dot{e}(s)ds \\
\geqslant & \frac{T_2}{T_M}e^T(t)\{\mathcal{G} + T_M\mathrm{sym}\{\eta_1\} + \mathcal{H}_1\}e(t) - \frac{T_2}{T_M}e^T(t)\{T_M\eta_1 + T_M\eta_2 + \mathcal{H}_1\}e(t_k) \\
& + \frac{T_2}{T_M}e^T(t_k)\{T_M\mathrm{sym}\{\eta_1\} + \mathcal{H}_1\}e(t_k) \\
\geqslant & \frac{T_2}{T_M}\chi_1^T(t)\mathcal{Q}\chi_1(t) > 0.
\end{aligned}
$$

Next, state evolution trajectories are estimated for each interval: the intermittent control interval $t \in [t_k, t_k + \mathscr{T}_k)$ and the uncontrolled interval $t \in [t_k + \mathscr{T}_k, t_{k+1})$.

When $t \in [t_k, t_k + \mathscr{T}_k)$,

$$
\begin{aligned}
D^+ T_2(t) & \int_{t_k}^t \int_\tau^t \dot{e}^T(s)\mathcal{H}_2\dot{e}(s)dsd\tau \\
= & \dot{T}_2(t)\int_{t_k}^t \int_\tau^t \dot{e}^T(s)\mathcal{H}_2\dot{e}(s)dsd\tau + T_2(t)\int_{t_k}^t \left[\frac{d}{dt}\int_\tau^t \dot{e}^T(s)\mathcal{H}_2\dot{e}(s)ds\right] \\
& + T_2(t)\{\dot{t}\int_\tau^t \dot{e}^T(s)\mathcal{H}_2\dot{e}(s)ds - \dot{t}_k\int_\tau^t \dot{e}^T(s)\mathcal{H}_2\dot{e}(s)ds\} \\
= & (t - t_k)T_2(t)\dot{e}^T(t)\mathcal{H}_2\dot{e}(t) - \int_{t_k}^t \int_\tau^t \dot{e}^T(s)\mathcal{H}_2\dot{e}(s)dsd\tau.
\end{aligned}
\tag{25}
$$

Then,

$$
\begin{aligned}
D^+ V(t) = & D^+ V_1(t) + D^+ V_2(t) + D^+ V_{\mathcal{X}} \\
= & 2e^T(t)\mathcal{G}\dot{e}(t) + T_2(t)\dot{e}^T(t)\mathcal{H}_1\dot{e}(t) - \int_{t_k}^t \dot{e}^T(s)\mathcal{H}_1\dot{e}(s)ds \\
& + T_1(t)T_2(t)\dot{e}^T(t)\mathcal{H}_2\dot{e}(t) - \int_{t_k}^t \int_\tau^t \dot{e}^T(s)\mathcal{H}_2\dot{e}(s)dsd\tau \\
& + 2T_2(t)\chi_1^T(t)\mathcal{B}\check{\chi}_1(t) - \chi_1^T(t)\mathcal{B}\chi_1(t).
\end{aligned}
\tag{26}
$$

It can be derived

$$
\begin{aligned}
D^+ V(t) + 2\epsilon V(t) = & 2e^T(t)\mathcal{G}\dot{e}(t) + 2\epsilon e^T(t)\mathcal{G}e(t) + T_2(t)\dot{e}^T(t)\mathcal{H}_1\dot{e}(t) \\
& + (2\epsilon T_2(t) - 1)\int_{t_k}^t \dot{e}^T(s)\mathcal{H}_1\dot{e}(s)ds \\
& + T_1(t)T_2(t)\dot{e}^T(t)\mathcal{H}_2\dot{e}(t) \\
& + (2\epsilon T_2(t) - 1)\int_{t_k}^t \int_\tau^t \dot{e}^T(s)\mathcal{H}_2\dot{e}(s)dsd\tau \\
& + 2T_2(t)\chi_1^T(t)\mathcal{B}\check{\chi}_1(t) + (2\epsilon T_2(t) - 1)\chi_1^T(t)\mathcal{B}\chi_1(t).
\end{aligned}
\tag{27}
$$

Divide the Formula (27) into parts and estimate.

$$2T_2(t)\chi_1^T(t)\mathcal{B}\check{\chi}_1(t) = 2T_2 e^T(t)(\eta_1 + \eta_1^T)\dot{e}(t) - 2T_2 e^T(t_k)(\eta_1 + \eta_2)^T \dot{e}(t). \tag{28}$$

According to the Wirtinger-type inequality of Lemma 3, one can obtained

$$(2\epsilon T_2(t) - 1)\int_{t_k}^t \dot{e}^T(s)\mathcal{H}_1\dot{e}(s)ds \leqslant \frac{(2\epsilon T_2(t) - 1)}{T_M}\chi_2(s)^T \Lambda_1 \chi_2(s), \tag{29}$$

$$(2\epsilon T_2(t) - 1)\int_{t_k}^t \int_\tau^t \dot{e}^T(s)\mathcal{H}_2\dot{e}(s)ds d\tau \leqslant (2\epsilon T_2(t) - 1)\chi_3(s)^T \Lambda_2 \chi_3(s), \tag{30}$$

where $\chi_2 = \mathrm{col}\{e(t), e(t_k), \rho(t)\}$ and $\chi_3 = \mathrm{col}\{e(t), \rho(t)\}, \rho(t) = \frac{1}{T_1(t)}\int_{t_k}^t e(s)ds$.
The matrices Λ_1 and Λ_2 are transformed into

$$\Lambda_1 = \begin{bmatrix} 4\mathfrak{G}_1 & 2\mathfrak{G}_1 & -6\mathfrak{G}_1 \\ * & 4\mathfrak{G}_1 & -6\mathfrak{G}_1 \\ * & * & 12\mathfrak{G}_1 \end{bmatrix}, \Lambda_2 = \begin{bmatrix} 2\mathfrak{G}_2 & -2\mathfrak{G}_2 \\ * & 2\mathfrak{G}_2 \end{bmatrix}.$$

Using (28)–(30), the Equation (27) can be transformed Into

$$\begin{aligned}
D^+V(t) + 2\epsilon V(t) \leqslant &\, 2e^T(t)\mathcal{G}\dot{e}(t) + 2\epsilon e^T(t)\mathcal{G}e(t) \\
&+ (2\epsilon T_2(t) - 1)\chi_1^T(t)\mathcal{B}\chi_1(t) + T_2(t)\dot{e}^T(t)\mathcal{H}_1\dot{e}(t) \\
&+ \frac{T_M}{4}T_1\dot{e}^T(t)\mathcal{H}_2\dot{e}(t) + \frac{T_M}{4}T_2\dot{e}^T(t)\mathcal{H}_2\dot{e}(t) \\
&+ 2T_2 e^T(t)(\eta_1 + \eta_1^T)\dot{e}(t) - 2T_2 e^T(t_k)(\eta_1 + \eta_2)^T \dot{e}(t) \\
&+ \frac{(2\epsilon T_2(t) - 1)}{T_M}\chi_2(s)^T \Lambda_1 \chi_2(s) \\
&+ (2\epsilon T_2(t) - 1)\chi_3(s)^T \Lambda_2 \chi_3(s).
\end{aligned} \tag{31}$$

For any $n \times n$ matrix $\mathscr{A}_i$, $i = 1, 2, 3$, one has

$$\begin{aligned}
2[e^T(t)\mathscr{A}_1 + \dot{e}^T(t)\mathscr{A}_2 + e^T(t_k)\mathscr{A}_3] \\
\times [(\alpha I - D)e(t) + E\hat{F}(e_i(t)) + \mathscr{W}e(t_k)(t) - \dot{e}(t)] = 0
\end{aligned} \tag{32}$$

When $t \in [\mathscr{T}_k, t_{k+1})$, the following inequality is similarly obtained

$$\begin{aligned}
D^+V(t) + 2\epsilon V(t) \leqslant &\, 2e^T(t)\mathcal{G}\dot{e}(t) + 2\epsilon e^T(t)\mathcal{G}e(t) \\
&+ (2\epsilon T_2(t) - 1)\chi_1^T(t)\mathcal{B}\chi_1(t) + T_2(t)\dot{e}^T(t, x)\mathcal{H}_1\dot{e}(t, x) \\
&+ \frac{T_M}{4}T_1\dot{e}^T(t)\mathcal{H}_2\dot{e}(t) + \frac{T_M}{4}T_2\dot{e}^T(t)\mathcal{H}_2\dot{e}(t) \\
&+ 2T_2 e^T(t)(\eta_1 + \eta_1^T)\dot{e}(t) - 2T_2 e^T(t_k)(\eta_1 + \eta_2)^T \dot{e}(t) \\
&+ \frac{(2\epsilon T_2(t) - 1)}{T_M}\chi_2(s)^T \Lambda_1 \chi_2(s) + (2\epsilon T_2(t) - 1)\chi_3(s)^T \Lambda_3 \chi_3(s).
\end{aligned} \tag{33}$$

For any $n \times n$ matrix $\mathscr{A}_i$ with $i = 4, 5, 6$, the following is established

$$\begin{aligned}
2[e^T(t)\mathscr{A}_4 + \dot{e}^T(t)\mathscr{A}_5 + e^T(t_k)\mathscr{A}_6] \\
\times [(\alpha I - D)e(t) + E\hat{F}(e_i(t)) - \dot{e}(t)] = 0.
\end{aligned} \tag{34}$$

By Assumption 1, there exists an arbitrary adapted dimensional diagonal matrix $P_2 > 0$ such that the inequality is established:

$$2\hat{F}^T(e(t))P_2[\hat{\Phi}e(t) - \hat{F}(e(t))] \geqslant 0. \tag{35}$$

According to the Equations (31)–(35), the following is established

$$D^+V(t) + 2\epsilon V(t) \leqslant \chi^T(t)\left[\frac{T_1(t)}{T_k}\mathscr{L}_1(T_k) + \frac{T_2(t)}{T_k}\mathscr{L}_2(T_k)\right]\chi(t). \tag{36}$$

where $\chi(t) = \text{col}\{e(t), e(t_k), \hat{F}(e_i(t)), \rho(t), \dot{e}(t)\}$.

From the linear matrix inequalities (LMIs) (16) and (17), it can be obtained

$$D^+V(t) + 2\epsilon V(t) < 0, \tag{37}$$

where

$$V(t) < \exp\{-2\epsilon(t - t_k)\}V(t_k), \; t \in [t_k, t_{k+1}), \tag{38}$$

and

$$e^T(t_{k+1})\mathcal{G}e(t_{k+1}) < \exp\{-2\epsilon T_k\}e^T(t_k)\mathcal{G}e(t_k). \tag{39}$$

It is estimated that at the saturation impulse moment $t = t_{k+1}$, by $e_i(t) = e^{\alpha t}\{\xi_i(t) - \omega_i(t)\}$.

$$v^T(t_{k+1})\mathcal{G}v(t_{k+1}) < \exp\{-2(\epsilon + \alpha)T_k\}v^T(t_k)\mathcal{G}v(t_k). \tag{40}$$

The stability analysis of the system (14) is discussed in three areas, accordingly.

Case 1. When $\epsilon + \alpha > 0$, the following can be obtained:

$$\begin{aligned} v^T(t_1^-)\mathcal{G}v(t_1^-) &\leqslant \exp\{-2(\epsilon + \alpha)T_k\}v^T(t_0)\mathcal{G}v(t_0) \\ &\leqslant \varpi\exp\{-2(\epsilon + \alpha)T_m\}. \end{aligned} \tag{41}$$

where $v(t_1^-) \in \mathcal{E}\{\mathcal{G}, \varpi\exp\{-2(\epsilon + \alpha)T_m\}\}$.

Based on the Schur complement theory obtained from the condition (18), it can be shown that

$$H_{(j)}^T H_{(j)} \leqslant \varpi^{-1}\bar{u}_0^2\exp\{-2(\epsilon + \alpha)T_m\}\mathcal{G}. \tag{42}$$

The trajectory of the error-system is

$$\begin{aligned} V(t_1) &= e^T(t_1, x)\mathcal{G}e(t_1, x) \\ &= e^T(t_1^-, x)\sum_1^{2^n}\varsigma_J\left(I + \mathscr{D}_J K + \mathscr{D}_J^- H\right)^T\mathcal{G}\sum_1^{2^n}\varsigma_J\left(I + \mathscr{D}_J K + \mathscr{D}_J^- H\right)e(t_1^-) \\ &\leqslant \pi e^T(t_1, x)\mathcal{G}e(t_1, x) = \pi V(t_1^-). \end{aligned} \tag{43}$$

Since $e(t) = \exp\{\alpha t\}v(t)$ and the condition (19), the following holds

$$v^T(t_1)\mathcal{G}v(t_1) < \pi v^T(t_1^-)\mathcal{G}v(t_1^-). \tag{44}$$

Using the same method, when $t_k = t_2^-$ is obtained:

$$\begin{aligned} v^T(t_2^-)\mathcal{G}v(t_2^-) &\leq \exp\{-2(\epsilon + \alpha)T_1\}v^T(t_1)\mathcal{G}v(t_1) \\ &\leq \exp\{-2(\epsilon + \alpha)T_m\}\pi v^T(t_1^-)\mathcal{G}v(t_1^-) \\ &\leq \varpi\exp\{-2(\epsilon + \alpha)T_m\}. \end{aligned} \tag{45}$$

Using mathematical induction, one can be drawn:

$$V(t_{k-1}) \leq \pi V(t_k^-). \tag{46}$$

From (18), it is possible to derive

$$V(t_k) \leq \pi V(t_k^-). \tag{47}$$

Furthermore, based on the assumption 3, we can obtain:

$$\frac{t - t_0}{T_M} - 1 \leqslant k \leqslant \frac{t - t_0}{T_m}, k \in \mathbb{N}_0. \tag{48}$$

Finally, from Equations (38) and (47), it follows that

$$
\begin{aligned}
V(t) &\leq \exp\{-2\epsilon(t - t_k)\}V(t_k) \\
&\leq \pi \exp\{-2\epsilon(t - t_k)\}V(t_k^-) \\
&\leq \cdots \\
&\leq \pi^k \exp\left\{-2\epsilon\left[(t - t_k) + \sum_{s=1}^{k-1} T_s\right]\right\}V(t_k^-) \\
&= \pi^k \exp\{-2\epsilon(t - t_0)\}V(t_0) \\
&\leq \pi^{\frac{t-t_0}{T_M} - 1}\exp\{-2\epsilon(t - t_0)\}V(t_0).
\end{aligned}
\tag{49}
$$

In summary, based on Equations (48) and (49), this means that

$$V(t) \leq \tilde{\pi} \exp\left\{\left(\frac{\ln \pi}{T_M} - 2\epsilon\right)(t - t_0)\right\}V(t_0), \tag{50}$$

where $\tilde{\pi} = \max\{\pi^{-1}, 1, \pi^{\frac{T_M}{T_m}}\}$.

Generally speaking,

$$\|v(t)\| \leq \sqrt{\frac{\tilde{\pi}\lambda_{\max}(\mathcal{G})}{\lambda_{\min}(\mathcal{G})}}\exp\left\{\left(\frac{\ln \pi}{2T_M} - \epsilon - \alpha\right)(t - t_0)\right\}\|v_i(t_0)\|. \tag{51}$$

Case 2. When $\epsilon + \alpha < 0$, we can easily obtain:

$$v^T\left(t_{k+1}^-\right)\mathcal{G}v\left(t_{k+1}^-\right) \leqslant \exp\{-2(\epsilon + \alpha)T_M\}v^T(t_k)\mathcal{G}v(t_k). \tag{52}$$

Thus, for $\forall v_i(t_0) \in \mathcal{E}\{\mathcal{G}, \varpi\}$, it follows that

$$v^T\left(t_1^-\right)\mathcal{G}v\left(t_1^-\right) \leqslant \exp\{-2(\epsilon + \alpha)T_M\}v^T(t_0)\mathcal{G}v(t_0). \tag{53}$$

Using the Schur complement theory with the condition (17), we have that

$$H_{(j)}^T H_{(j)} \leqslant \varpi^{-1}\bar{u}_0^2\exp\{-2(\epsilon + \alpha)T_M\}\mathcal{G}. \tag{54}$$

Similar to the proof process for case 1, using mathematical induction, we can conclude the following

$$
\begin{aligned}
V(t) &\leq \pi^k \exp\{-2\epsilon(t - t_0)\}V(t_0) \\
&\leq \pi^{-1}\exp\left\{\left(\frac{\ln \pi}{T_M} - 2\epsilon\right)(t - t_0)\right\}V(t_0).
\end{aligned}
\tag{55}
$$

In summary, it can be concluded that

$$\|v(t)\| \leq \sqrt{\frac{\lambda_{\max}(\mathcal{G})}{\pi\lambda_{\min}(\mathcal{G})}} \times \exp\left\{\left(\frac{\ln \pi}{2T_M} - \epsilon - \alpha\right)(t - t_0)\right\}\|v_i(t_0)\|. \tag{56}$$

Case 3. When $\epsilon + \alpha = 0$, based on Equation (37), there exists a very small constant $\beta \in (0, -\epsilon)$ which, due to the continuity of (37), makes the following hold

$$D^+V(t) + 2(\epsilon + \beta)V(t) < 0,$$

this means

$$V(t) \leq \exp\{-2(\epsilon + \beta)(t - t_k)\}V(t_k), \ t \in [t_k, \ t_{k+1}). \tag{57}$$

Thus, similar to case 1, one can infer that

$$V(t) \leq \pi V(t_k), \ t \in [t_k, \ t_{k+1}). \tag{58}$$

Since (57) and (58), it follows that

$$\|v(t)\| \leq \sqrt{\frac{\tilde{\pi}\lambda_{\max}(\mathcal{G})}{\lambda_{\min}(\mathcal{G})}} \times \exp\left\{\left(\frac{\ln \pi}{2T_M} - \epsilon\right)(t - t_0)\right\}\|v(t_0)\|.$$

□

Remark 5. *In the proof process, a* Lyapunov–Krasovskii *generalised function related to the time state is devised, and the $\mathcal{B}$ matrix term is widely used in existing proofs in the literature. In addition, we set two integral terms $T_2(t) \int_{t_k}^{t} \dot{e}^T(s)\mathcal{H}_1\dot{e}(s)ds$ and $T_2(t) \int_{t_k}^{t} \int_{\tau}^{t} \dot{e}^T(s)\mathcal{H}_2\dot{e}(s)ds d\tau$ to obtain more relaxed conditions.*

When the input saturation term is ignored, the error system (14) can be rewritten as

$$\begin{cases} \dot{e}_i(t) = (\alpha I - D)e(t) + E\hat{F}(e_i(t)) + \mathcal{W}e(t_k), \ t \in [t_k, \ t_k + \mathcal{T}_k), \\ \dot{e}_i(t) = (\alpha I - D)e(t) + E\hat{F}(e_i(t)), \ t \in [t_k + \mathcal{T}_k, \ t_{k+1}), \\ \Delta e(t_{k+1}, x) = Ke\left(t_{k+1}^-\right), \ t = t_{k+1}. \end{cases} \tag{59}$$

Corollary 1. *For a given constant $T_M > T_m \geqslant 0$, $\varpi > 0$, $\epsilon > 0$, $\alpha > 0$, $0 < \pi < e^{2T_M(\epsilon + \alpha)}$, and a given $n \times n$ dimensional matrix K, $\mathcal{W}$ and D. Suppose that for $T_K \in \{T_m, T_M\}$, there exist diagonal matrices $P_2 \in \mathbb{R}^{n \times n}$, matrices $\mathcal{G} > 0$, $n \times n$ matrices $\mathcal{H}_1, \mathcal{H}_2, \eta_1, \eta_2 \in \mathbb{R}^{n \times n}$, $\mathscr{A}_i, i = 1, ..., 6$, linear matrix inequality (15)–(17), the following inequality is established*

$$\begin{bmatrix} -\pi\mathcal{G} & (I + K)^T \mathcal{G} \\ \star & -\mathcal{G} \end{bmatrix} \leq 0. \tag{60}$$

Then, the trajectory of the dynamical system (59) achieve stability at $-\frac{\ln \pi}{2T_M} + \alpha + \epsilon$ decay rate exponentially.

3.2. Synchronisation Analysis Based on SNA

By Lemma 4, the dead-zone nonlinearity $\mathscr{R}(U(t_k)) = U(t_k) - \text{Sat}\{U(t_k)\}$ is defined, where $\mathscr{R}(U(t_k, \ x)) = [\mathscr{R}(U_1(t_k, \ x)), \mathscr{R}(U_2(t_k, \ x)), \cdots, \mathscr{R}(U_n(t_k, \ x))]$. Thus, the error system is transformed into

$$\begin{cases} \dot{e}_i(t) = (\alpha I - D)e(t) + E\hat{F}(e_i(t)) + \mathcal{W}e(t_k), \ t \in [t_k, \ t_k + \mathcal{T}_k), \\ \dot{e}_i(t) = (\alpha I - D)e(t) + E\hat{F}(e_i(t)), \ t \in [t_k + \mathcal{T}_k, \ t_{k+1}), \\ \Delta e(t_{k+1}) = Ke(t_{k+1}^-) - \mathscr{R}(Ke(t_{k+1}^-)), \ t = t_{k+1}. \end{cases} \tag{61}$$

If $e(t_k^-) \in \pounds(KH)$, based on Lemma 4, the following condition establishes with respect to nonlinear functions

$$\mathscr{R}^T(Ke(t_{k+1}^-))P_1\left[\mathscr{R}(Ke(t_{k+1}^-)) - He(t_{k+1}^-)\right] \leq 0. \tag{62}$$

Theorem 2. *Given the constants $T_M > T_m \geqslant 0$, $\varpi > 0$, $\pi > 0$, $\alpha > 0$, and $\epsilon \leqslant 0$, and given the matrices $H, K, \mathcal{W}, D \in \mathbb{R}^{n \times n}$. Suppose that there exist dimensional diagonal matrices $P_1 \in \mathbb{R}^{n \times n} > 0$ and $P_2 \in \mathbb{R}^{n \times n} > 0$, matrices $\mathcal{G} > 0$, $n \times n$ dimensional matrices $\bar{\mathcal{H}}_1, \bar{\mathcal{H}}_2, \eta_1$, and $\eta_2, \mathscr{A}_i, i = 1, \ldots, 6$.*

Then, for any of initial value $v(t_0) \in \mathcal{E}\{\mathcal{G}, \varpi\}$, $T_k \in \{T_m, T_M\}$ the following conditions hold:

(1) *if* $\alpha > -\epsilon, 0 < \pi < \exp\{2(\epsilon + \alpha)T_m\}$, *linear matrix inequality* (15)–(17), *the following linear matrix inequality holds*

$$\begin{bmatrix} \mathcal{G} & (K_{(j)} - H_{(j)})^T \\ \star & \omega^{-1}\bar{u}_0^2 \exp\{-2(\epsilon + \alpha)T_m\} \end{bmatrix} \geq 0, \tag{63}$$

$$\mathcal{O} = \begin{bmatrix} \mathcal{O}_1 & \mathcal{O}_2 \\ \star & \mathcal{O}_3 \end{bmatrix} \geq 0. \tag{64}$$

The error system (61) *would achieve stability with an exponential decay rate* $-\frac{\ln \pi}{2T_M} + \epsilon + \alpha$.

(2) *If* $0 < \alpha < -\epsilon, 0 < \pi < \exp\{2(\epsilon + \alpha)T_m\}$, *linear matrix inequality* (15)–(17), (64), *and the following linear matrix inequality holds*

$$\begin{bmatrix} \mathcal{G} & (K_{(j)} - H_{(j)})^T \\ * & \omega^{-1}\bar{u}_{(0)}^2 \exp\{-2(\epsilon + \alpha)T_M\} \end{bmatrix} \geq 0. \tag{65}$$

The error system (61) *would achieve stability at an exponential decay rate* $-\frac{\ln \pi}{2T_M} + \epsilon + \alpha$.

(3) *If* $\alpha + \epsilon = 0$, *there exists a sufficiently small constant* $\beta \in (0, -\epsilon)$ *such that* $0 < \pi < \exp\{2(\epsilon + \alpha)T_m\}$ *holds. Then the error system* (61) *would achieve stability with an exponential decay rate* $(-\frac{\ln \pi}{2T_M}, -\frac{\ln \pi}{2T_M} + \epsilon)$.

That is, for all initial errors $\mathcal{E}\{\mathcal{G}, \omega\}$ *in the ellipsoid, the response system* (6) *and the driving system* (5) *are locally exponentially synchronised under hybrid control. Therefore, the estimated domain of attraction is* $R_A = \mathcal{E}\{\mathcal{G}, \omega\}$.

Proof of Theorem 2. The above part of the proof is similar to Theorem 1 and is omitted. If the linear matrix inequalities (16) and (17) hold.

Then, since $e(t) = \exp\{\alpha t\}v(t)$ when

$$v^T\left(t_{k+1}^-\right)\mathcal{G}v\left(t_{k+1}^-\right) < \exp\{-2(\epsilon + \alpha)T_k\}v^T(t_k)\mathcal{G}v(t_k). \tag{66}$$

Case 1. When $\epsilon + \alpha > 0$, it can be obtained:

$$\begin{aligned} v^T\left(t_1^-\right)\mathcal{G}v\left(t_1^-\right) &\leq \exp\{-2(\epsilon + \alpha)T_k\}v^T(t_0)\mathcal{G}v(t_0) \\ &\leq \omega \exp\{-2(\epsilon + \alpha)T_k\}, \end{aligned} \tag{67}$$

Furthermore, from the Schur complement theory of Equation (63), it follows:

$$\left(K_{(j)} - H_{(j)}\right)^T\left(K_{(j)} - H_{(j)}\right) \leqslant \omega^{-1}\bar{u}_0^2 \exp\{-2(\epsilon + \alpha)T_m\}\mathcal{G}. \tag{68}$$

Then, for $\forall v(t_0) \in \mathcal{E}\{\mathcal{G}, \omega\}$, there exists $v(t_1^-, x) \in \pounds(KH)$ that holds.

This can be obtained from the linear matrix inequalities (64) and (62)

$$\begin{aligned} V(t_1) &= e^T(t_1)\mathcal{G}e(t_1) \\ &\leq [(I + K)e(t_1^-) - \mathscr{R}(Ke(t_1^-))]^T\mathcal{G}[(I + K)e(t_1^-) - \mathscr{R}(Ke(t_1^-))] \\ &\quad - \mathscr{R}^T(Ke(t_1^-))P_1[\mathscr{R}(Ke(t_1^-)) - He(t_1^-)] \\ &= \chi_4^T(t_1^-)\mathcal{O}\chi_4(t_1^-) + \pi e^T(t_1^-)\mathcal{G}e(t_1^-) \leq \pi e^T(t_1^-)\mathcal{G}e(t_1^-). \end{aligned} \tag{69}$$

where $\chi_4(t, x) = \text{col}\{e(t), \mathscr{R}(Ke(t))\}$.

Using mathematical induction, from the linear matrix inequalities (64) and (62), it yields that

$$
\begin{aligned}
V(t_k) =& e^T(t_k)\mathcal{G}e(t_k) \\
\leq& [(I+K)e(t_k^-) - \mathscr{R}(Ke(t_k^-))]^T \mathcal{G}[(I+K)e(t_k^-) - \mathscr{R}(Ke(t_k^-))] \\
& - \mathscr{R}^T(Ke(t_k^-))P_1[\mathscr{R}(Ke(t_k^-)) - He(t_k^-)] \\
=& \chi_4^T(t_k^-)\mathcal{O}\chi_4(t_k^-) + \pi e^T(t_k^-)\mathcal{G}e(t_k^-) \leq \pi e^T(t_k^-)\mathcal{G}e(t_k^-).
\end{aligned}
\tag{70}
$$

When $t \in [t_k, t_{k+1})$, the following inequality establishes according to Equations (38) and (70)

$$
\begin{aligned}
V(t) \leq& \exp\{-2\epsilon(t-t_k)\}V(t_k) \\
\leq& \pi \exp\{-2\epsilon(t-t_k)\}V(t_k^-) \\
\leq& ... \\
\leq& \pi^k \exp\{-2\epsilon(t-t_0)\}V(t_0).
\end{aligned}
\tag{71}
$$

Similarly to Theorem 1, one obtains

$$
V(t) \leq \tilde{\pi}\exp\left\{\left(\frac{\ln\pi}{T_M} - 2\epsilon\right)(t-t_0)\right\}V(t_0),
\tag{72}
$$

where $\tilde{\pi} = \max\left\{\pi^{-1},\ 1,\ \pi^{\frac{T_M}{T_m}}\right\}$.

Thus, one can obtain

$$
\|\nu(t)\| \leq \sqrt{\frac{\tilde{\pi}\lambda_{\max}(\mathcal{G})}{\lambda_{\min}(\mathcal{G})}}\exp\left\{\left(\frac{\ln\pi}{2T_M} - \epsilon - \alpha\right)(t-t_0)\right\}\|\nu_i(t_0,x)\|.
\tag{73}
$$

Case 2. When $\epsilon + \alpha < 0$, it is obtained that

$$
\nu^T(t_1^-)\mathcal{G}\nu(t_1^-) < \exp\{-2(\epsilon+\alpha)T_M\}\nu^T(t_0)\mathcal{G}\nu(t_0).
\tag{74}
$$

Furthermore, from the Schur complement theory of Equation (63), we have that

$$
\left(K_{(j)} - H_{(j)}\right)^T\left(K_{(j)} - H_{(j)}\right) \leqslant \varpi^{-1}\bar{u}_0^2\exp\{-2(\epsilon+\alpha)T_m\}\mathcal{G}.
\tag{75}
$$

Thus, for $\nu(t_0) \in \mathcal{E}\{\mathcal{G},\ \varpi\exp\{-2(\epsilon+\alpha)T_M\}\}$, there are

$$
\begin{aligned}
& \nu^T(t_1^-)\left(K_{(j)} - H_{(j)}\right)^T\left(K_{(j)} - H_{(j)}\right)\nu^T(t_1^-) \\
& \leq \varpi^{-1}\bar{u}_0^2\exp\{-2(\epsilon+\alpha)T_m\}\nu^T(t_1^-)\mathcal{G}\nu^T(t_1^-) \\
& \leq \varpi^{-1}\bar{u}_0^2\nu^T(t_0)\mathcal{G}\nu^T(t_0) \\
& \leq \bar{u}_0^2,
\end{aligned}
$$

and

$$
\mathscr{R}^T(Ke(t_k^-))P_1[\mathscr{R}(Ke(t_k^-)) - He(t_k^-)] \leq 0.
\tag{76}
$$

Same as Case 1, which gives

$$
V(t_k) \leq \pi V(t_k^-),
\tag{77}
$$

It can be concluded that

$$
\|\nu(t)\| \leq \sqrt{\frac{\lambda_{\max}(\mathcal{G})}{\pi\lambda_{\min}(\mathcal{G})}}\exp\left\{\left(\frac{\ln\pi}{2T_M} - \epsilon - \alpha\right)(t-t_0)\right\}\|\nu(t_0)\|.
\tag{78}
$$

Case 3. When $\epsilon + \alpha = 0$, the analysis is similar to Theorem 1. Omitted. □

4. Numerical Simulation

Consider a CNNs model of three neuron nodes (5) with the following parameter settings

$$D = I_3, \ E = \begin{bmatrix} 1.2 & -1.6 & 0 \\ 1.25 & 1 & 0.9 \\ 0 & 2.2 & 1.5 \end{bmatrix} \ (5)$$

And the activation function $F(\xi_i) = [F_1(\xi_1), F_2(\xi_2), \cdots, F_n(\xi_n)]^T \in \mathbb{R}^n$, $F_i(\xi_i) = 0.5(\xi_i + 1| - |\xi_i - 1|)$, then $F_i(\xi_i)$ satisfies Assumption 1.

Setting the initial state of the system as $\xi_0 = [1.7, \ 2.4, \ -3.3]$, we can obtain the chaotic behaviour of the driving system (5) as shown in Figure 1 and dynamics trajectory of neuron as shown in Figure 2.
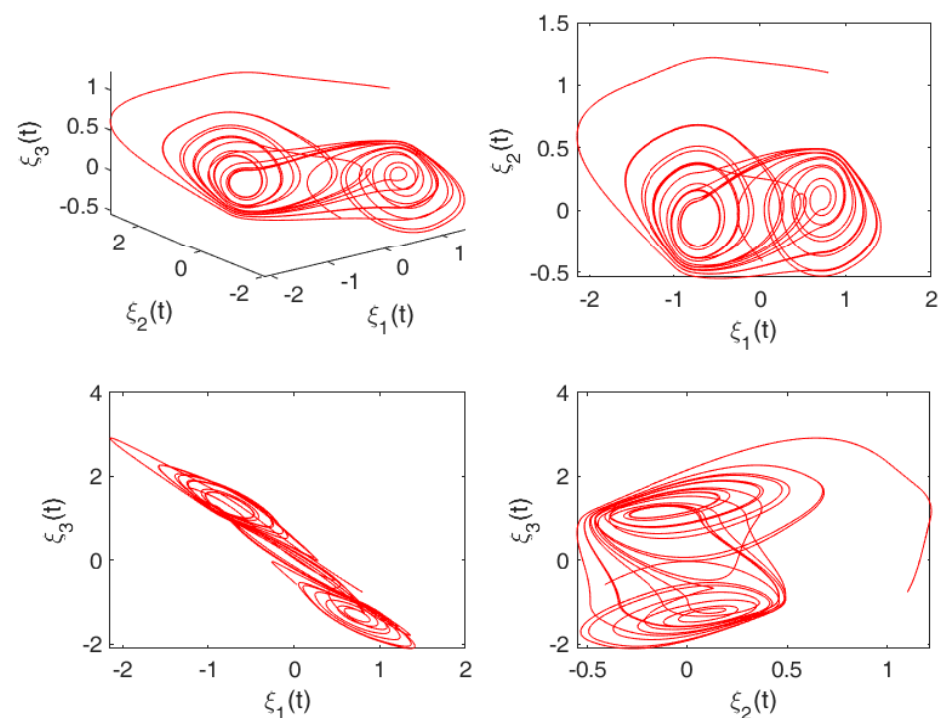
Figure 1. Driven system with initial value $\xi_0 = [1.7, \ 2.4, -3.3]$ (5) Chaotic behaviour.

Next, in order to synchronise the drive system (5) with the response system (6), consider the saturated pulse-interval controller (7), set the following parameters: $\alpha = 0.3$, $K = -0.5I_3$.

Take $\alpha = 0.4$, $\epsilon = -0.2$, $\varpi = 0.4$, $\pi = 0.9$ and $\varsigma = 0.6$. It can be introduced that $0 < \alpha < \epsilon$, and according to Theorem 1 and the LMIs toolbox, it can be proved that the linear matrix inequalities (15)–(19) are feasible solutions, and

$$\mathcal{G}_1 = 1.0 \times 10^3 \times \begin{bmatrix} 1.0497 & -0.6549 & 0.7531 \\ -0.6549 & 1.3659 & -0.9377 \\ 0.7531 & -0.9377 & 1.0417 \end{bmatrix},$$
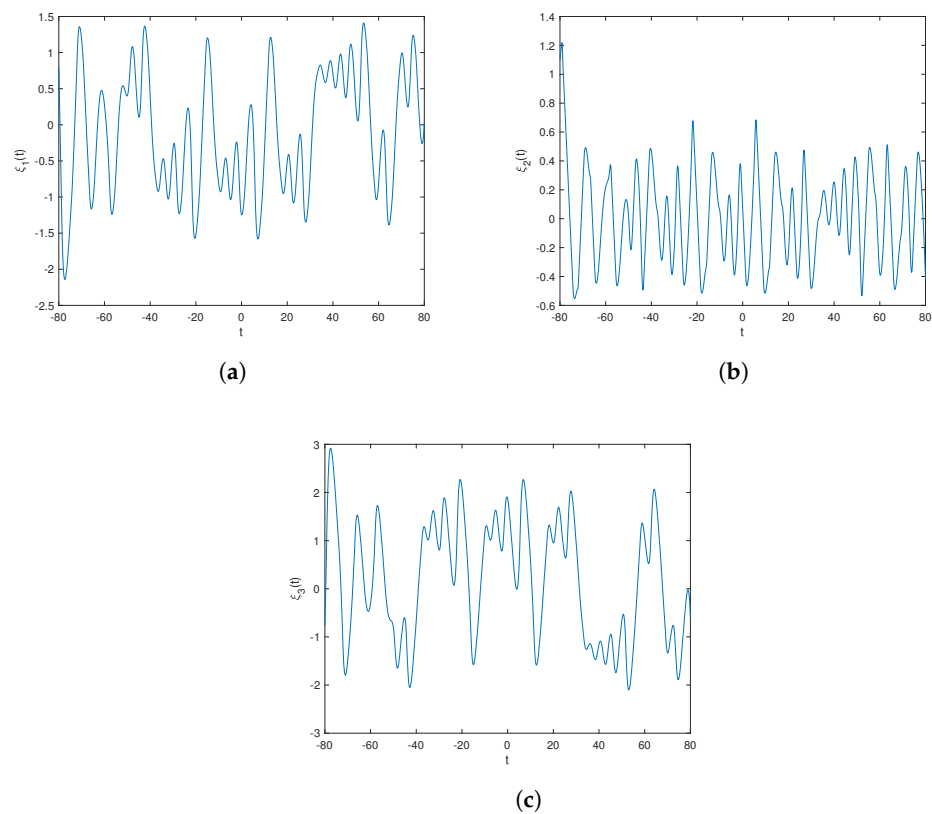
(a)

(b)

(c)

Figure 2. The evolutionary trajectories with initial values of $\xi_0 = [0.8, \ 1.1, \ -0.76]$: (**a**) ξ_1 evolutionary trajectory; (**b**) ξ_2 evolutionary trajectory; (**c**) ξ_3 evolutionary trajectory.

From Theorem 1, the synchronisation of the system (5) and the system (6) under saturated impulse-intermittent control is shown in Figure 3a. In the case of an inter-pulse controller without saturation, the driving system (5) and the response system (6) are synchronised as presented in Figure 3b. When the saturation parameter is reduced, the synchronisation of the drive system (5) and the response system (6) is shown in Figure 3c. Table 1 gives the details of the parameters to more clearly see the pattern of change in the evolutionary trajectory of the error system when we fix a parameter and change another parameter. This also better illustrates the feasibility of the controller we have designed. At the same time, we can derive the estimation of the admissible set $\mathcal{E}_1\{\mathcal{G}_1, \ 2\}$ of the initial value conditions of the error system (14) as shown in red in Figure 4.

Table 1. Comparison of control parameters in Figure 3.

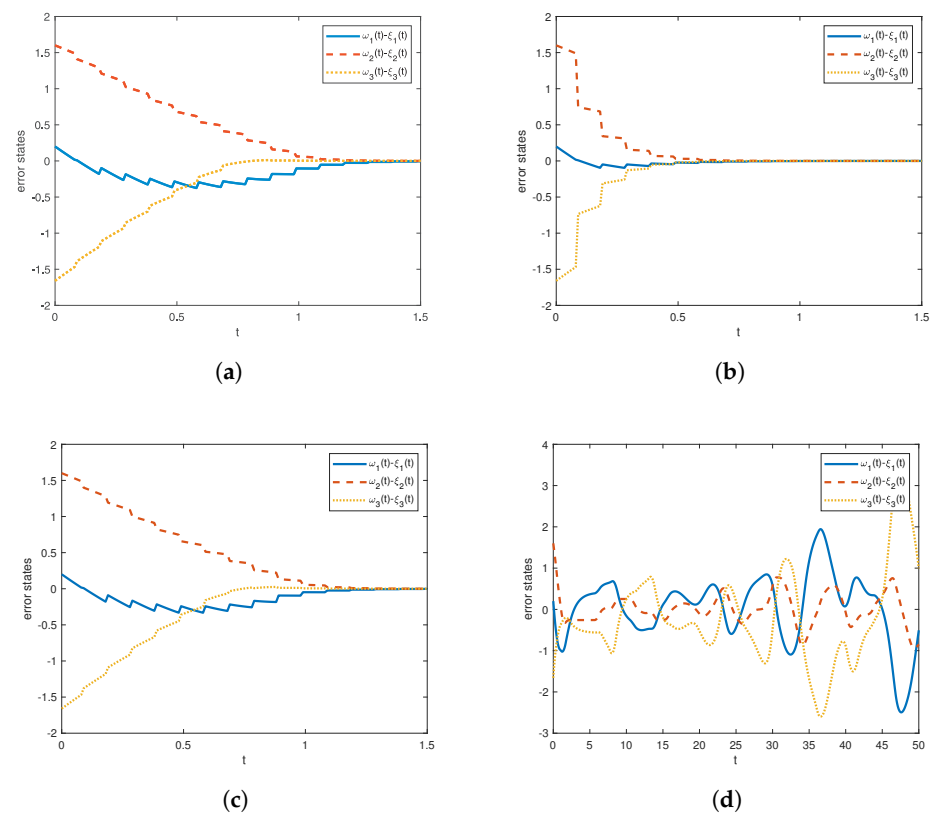| Title	Impulsive Gain	Intermittent Gain	Saturation Level
Figure 3a	-0.5	0.4	0.6
Figure 3b	-0.5	0.4	None
Figure 3c	-0.5	0.4	0.8
Figure 3d	0	0.4	None

Figure 3. Evolutionary trajectories of the error system in the controller (7): (**a**) Evolutionary trajectory of the error system with saturated impulse intermittent control; (**b**) Evolutionary trajectory of the error system with impulse intermittent control (14); (**c**) Evolutionary trajectory of the error system with varying saturation parameter impulse intermittent control. (**d**) Evolutionary trajectory of the error system (14) without impulse action

Fixing the control parameters constant, by solving the LMIs (15)–(17), (63) and (64) in Theorem 2, it can be seen that the linear matrix inequality has a feasible solution and the initial value conditions of the error system (14) can be solved. (64) show that the linear matrix inequality has a feasible solution and that the error system (14) The estimation of the admissible set $\mathcal{E}_2\{\mathcal{G}_2, 2\}$ of the initial value conditions is shown in blue in Figure 4.

$$\mathcal{G}_2 = 1.0 \times 10^3 \times \begin{bmatrix} 1.4641 & -0.5240 & 0.7590 \\ -0.5240 & 1.7305 & -0.9476 \\ 0.7590 & -0.9476 & 1.2149 \end{bmatrix}.$$

From Figure 4, it can be seen that the admissible sets of the error system when the initial conditions are constant are $\mathcal{E}_1\{\mathcal{G}_1, 2\}$ and $\mathcal{E}_2\{\mathcal{G}_2, 2\}$ satisfy $\mathcal{E}_1\{\mathcal{G}_1, 2\} \subset \mathcal{E}_2\{\mathcal{G}_2, 2\}$. It can be shown that the stabilisation conditions Theorem 1 is much less conservative.

Removing the impulse control under the set parameters leads to a system evolution trajectory as shown in the graph of Figure 3d and the comparison of parameters as shown in Figure 3a,d in Table 1, where we can see that purely intermittent control is unable to drive the response system to state synchronisation under this parameter. This also concludes the feasibility of our designed saturated pulse intermittent controller.
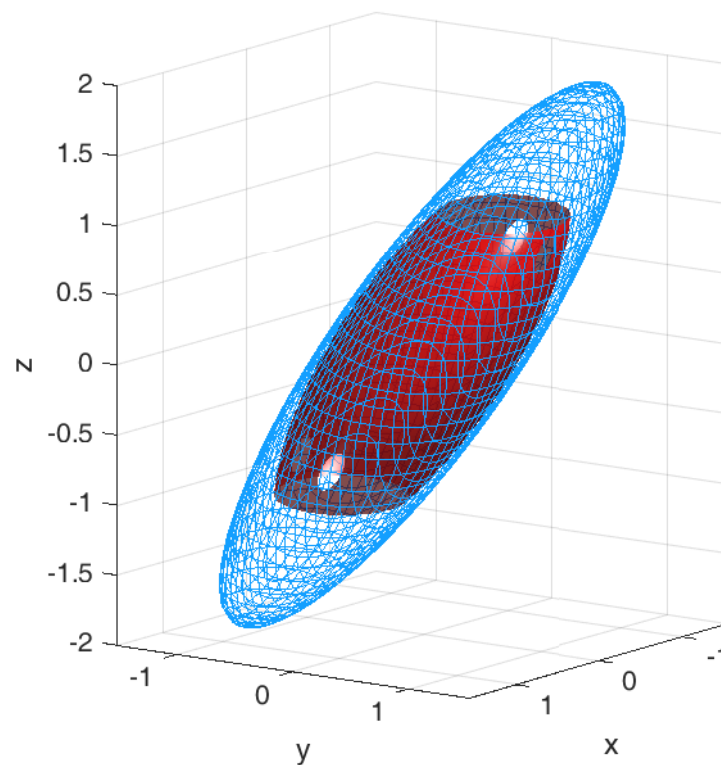
Figure 4. Theorem-1 and Theorem-2 Initial Value Conditional Estimates of the domains of attraction $\mathcal{E}_1\{\mathcal{G}_1,\ 2\}$ and $\mathcal{E}_2\{\mathcal{G}_2,\ 2\}$ where the red part represents the domain of attraction $\mathcal{E}_1\{\mathcal{G}_1,\ 2\}$, and the blue part represents the domain of attraction $\mathcal{E}_2\{\mathcal{G}_2,\ 2\}$.

5. Conclusions

The paper focuses on the impulse synchronisation of CNNs based on intermittent control and actuator saturation. The saturation function of the system is handled using a polyhedral representation, and the local stability conditions of the error system and the domain of attraction estimates are obtained by constructing suitable state-dependent Lyapunov–Krasovskii generalised functions in combination with Jensen's inequality, Wirtinger-type inequality, Schur complementary elicitation, Lyapunov stability theory, and the comparison principle. Finally, the validity of the obtained results is verified by numerical simulations. Using both methods, a less conservative stability criterion was obtained. The experimental simulation shows that the LMI calculation is simpler and consumes less energy. In our future work, we will incorporate more practical hybrid controllers into the chaotic neural network model, combine state-dependent saturated impulse control with event-triggered control, adaptive control, etc., and study its dynamic behavior.

Author Contributions: Conceptualisation, Z.C., C.L. and M.-F.L.; methodology, Z.C. and C.L.; software, Z.C.; validation, Z.C., C.L. and M.-F.L.; formal analysis, Z.C.; investigation, Z.C.; resources, Z.C. and C.L.; writing—original draft preparation, Z.C.; writing—review and editing, Z.C. and C.L.; supervision, M.-F.L. All authors have read and agreed to the published version of the manuscript.

Data Availability Statement: No new data were created or analysed in this study. Data sharing is not applicable to this article.

Conflicts of Interest: The authors declare no conflict of interest.

Abbreviations

The following abbreviations are used in this manuscript:

LMIs	Linear Matrix Inequality
PRs	Polyhedral Representations
SNA	Sector Non-linear Approach
CNNs	Chaotic Neural Networks
NNs	Neural Networks
SVSF	Standard Vector-valued Saturation Function

References

1. Che, H.; Wang, J. A two-timescale duplex neurodynamic approach to mixed-integer optimization. *IEEE Trans. Neural Netw. Learn. Syst.* **2020**, *32*, 36–48. [CrossRef] [PubMed]
2. Liu, C.; Wu, S.; Li, R.; Jiang, D.; Wong, H.S. Self-supervised graph completion for incomplete multi-view clustering. *IEEE Trans. Knowl. Data Eng.* **2023**, *35*, 9394–9406. [CrossRef]
3. Yuen, M.C.; Ng, S.C.; Leung, M.F.; Che, H. A metaheuristic-based framework for index tracking with practical constraints. *Complex Intell. Syst.* **2022**, *8*, 4571–4586. [CrossRef]
4. Liu, L.; Lei, M.; Bao, H. Event-triggered quantized quasisynchronization of uncertain quaternion-valued chaotic neural networks with time-varying delay for image encryption. *IEEE Trans. Cybern.* **2022**, *53*, 3325–3336. [CrossRef] [PubMed]
5. Wu, Y.; Zeng, J.; Dong, W.; Li, X.; Qin, D.; Ding, Q. A novel color image encryption scheme based on hyperchaos and hopfield chaotic neural network. *Entropy* **2022**, *24*, 1474. [CrossRef] [PubMed]
6. Lin, H.; Wang, C.; Sun, Y.; Wang, T. Generating-scroll chaotic attractors from a memristor-based magnetized hopfield neural network. *IEEE Trans. Circuits Syst. II Express Briefs.* **2022**, *70*, 311–315. [CrossRef]
7. Chen, X.; Cao, B.; Pouramini, S. Energy cost and consumption reduction of an office building by Chaotic Satin Bowerbird Optimization Algorithm with model predictive control and artificial neural network: A case study. *Energy* **2023**, *270*, 126874. [CrossRef]
8. Ma, M.; Xiong, K.; Li, Z.; Sun, Y. Dynamic behavior analysis and synchronization of memristor-coupled heterogeneous discrete neural networks. *Mathematics* **2023**, *11*, 375. [CrossRef]
9. Che, H.; Wang, J. A collaborative neurodynamic approach to global and combinatorial optimization. *Neural Netw.* **2019**, *114*, 15–27. [CrossRef]
10. Liu, C.; Li, R.; Wu, S.; Che, H.; Jiang, D.; Yu, Z.; Wong, H.S. Self-guided partial graph propagation for incomplete multiview clustering. *IEEE Trans. Neural Netw. Learn. Syst.* **2023** . [CrossRef]
11. Pan, B.; Li, C.; Che, H.; Leung, M.F.; Yu, K. Low-rank tensor regularized graph fuzzy learning for multi-view data processing. *IEEE Trans. Consum. Electron.* **2023** . [CrossRef]
12. Lu, W.; Chen, T. Synchronization of coupled connected neural networks with delays. *IEEE Trans. Circuits Syst. I Regul. Pap.* **2004**, *51*, 2491–2503. [CrossRef]
13. Li, X.; Cao, J. Adaptive synchronization for delayed neural networks with stochastic perturbation. *Phys. Lett. A* **2023**, *353*, 318–325. [CrossRef]
14. Wu, Z.; Shi, P.; Su, H.; Chu, J. Stochastic synchronization of markovian jump neural networks with time-varying delay using sampled data. *IEEE Trans. Cybern.* **2013**, *43*, 1796–1806. [CrossRef] [PubMed]
15. Li, N.; Zheng, W. Bipartite synchronization for inertia memristorbased neural networks on coopetition networks. *Neural Netw.* **2020**, *124*, 39–49. [CrossRef] [PubMed]
16. Wang, L.; Li, X.; ORegan, D. On the stability of impulsive functional differential equations with infinite delays. *Math. Methods Appl. Ences* **2015**, *38*, 3130–3140.
17. Leung, M.F.; Wang, J.; Li, D. Decentralized robust portfolio optimization based on cooperative-competitive multiagent systems. *IEEE Trans. Cybern.* **2022**, *52*, 12785–12794. [CrossRef]
18. Li, C.; Wu, S.; Feng, G.; Liao, X. Stabilizing effects of impulses in discrete-time delayed neural networks. *IEEE Trans. Neural Netw.* **2011**, *22*, 323–329. [CrossRef]
19. Li, C.; Feng, G.; Huang, T. On hybrid impulsive and switching neural networks. *IEEE Trans. Syst. Man Cybern. Part* **2019**, *38*, 1549–1560.
20. Lu, J.; Ho, D.W.C.; Cao, J.; Kurths, J. Exponential synchronization of linearly coupled neural networks with impulsive disturbances. *IEEE Trans. Neural Netw.* **2011**, *22*, 329–336. [CrossRef]
21. Wu, Y.; Sun, Z.; Ran, G.; Xue, L. Intermittent control for fixed-time synchronization of coupled networks. *IEEE/CAA J. Autom. Sin.* **2023**, *6*, 1488–1490. [CrossRef]
22. Zhong, Q.; Han, S.; Shi, K.; Zhong, S.; Kwon, O.M. Co-design of adaptive memory event-triggered mechanism and aperiodic intermittent controller for nonlinear networked control systems. *IEEE Trans. Circuits Syst. II Express Briefs* **2022**, *69*, 4979–4983. [CrossRef]
23. Lu, B.; Jiang, H.; Hu, C.; Abdurahman, A. Synchronization of hybrid coupled reaction-diffusion neural networks with time delays via generalized intermittent control with spacial sampled-data. *Neural Netw.* **2018**, *1005*, 75–87. [CrossRef] [PubMed]

24. Chen, B.; Hu, J.; Zhao, Y.; Ghosh, B.K. Finite-time velocity-free rendezvous control of multiple AUV systems with intermittent communication. *IEEE Trans. Syst. Man, Cybern. Syst.* **2022**, *52*, 6618–6629. [CrossRef]

25. Guo, Y.; Duan, M.; Wang, P. Input-to-state stabilization of semilinear systems via aperiodically intermittent event-triggered control. *IEEE Trans. Control Netw. Syst.* **2022**, *9*, 731–741. [CrossRef]

26. Hu, T.; Lin, Z. *Control Systems with Actuator Saturation: Analysis and Design*; Birkhauser: Basel, Switzerland, 2001.

27. Hu, T.; Lin, Z.; Chen, B. An analysis and design method for linear systems subject to actuator saturation and disturbance. *Automatica* **2002**, *38*, 351–359. [CrossRef]

28. Han, X.; Ma, Y.; Fu, L. Finite-time dynamic output-feedback dissipative control for singular uncertainty T–S fuzzy systems with actuator saturation and output constraints - ScienceDirect. *J. Frankl. Inst.* **2020**, *357*, 4543–4573. [CrossRef]

29. Qi, W.; Gao, X.; Kao, Y.; Lian, L.; Chen, Z. Observer design for stochastic time-delayed Markovian jump systems with incomplete transition rates and actuator saturation. *Optim. Control Appl. Methods* **2020**, *41*, 239–252. [CrossRef]

30. Aghayan, Z.; Alfi, A.; Machado, J. Robust stability analysis of uncertain fractional order neutral-type delay nonlinear systems with actuator saturation. *Appl. Math. Model.* **2021**, *90*, 1035–1048. [CrossRef]

31. Li, L.; Li, C.; Zhang, W. Delayed-impulsive control for difference systems with actuator saturation and its synchronisation application. *IET Control Theory Appl.* **2019**, *13*, 1129–1136. [CrossRef]

32. Li, H.; Li, C.; Ouyang, D.; Nguang, S.K. Impulsive synchronization of unbounded delayed inertial neural networks with actuator saturation and sampled-data control and its application to image encryption. *IEEE Trans. Neural Netw. Learn. Syst.* **2020**, *99*, 1460–1473. [CrossRef] [PubMed]

33. Li, H.; Li, C.; Huang, J. A hybrid impulsive and sampled-data control framework for a class of nonlinear dynamical systems with input constraints. *Nonlinear Anal. Hybrid Syst.* **2023**, *36*, 100881. [CrossRef]

34. Li, H.; Li, C.; Ouyang, D.; Nguang, S.K. Impulsive stabilization of nonlinear time-delay system with input saturation via delay-dependent polytopic approach. *IEEE Trans. Syst. Man Cybern. Syst.* **2020**, *99*, 7087–7098. [CrossRef]

35. Xiang, Z.; Li, Y.; Song, X. Dynamic analysis of a pest management SEI model with saturation incidence concerning impulsive control strategy. *Nonlinear Anal. Real World Appl.* **2009**, *10*, 2335–2345. [CrossRef]

36. Chen, W.-H.; Li, D.X.; Cao, D.Q. Robust Exponential Stability of Linear Impulsive Systems with input Saturation. *J. Guangxi Univ. Natl. (Natural Sci. Ed.* **2000**, *1*, 128–135.

37. Hur, J.; Lee, M.; Kim, D.; Park, P. A Variable Step-Size Robust Saturation Algorithm Against Impulsive Noises. *IEEE Trans. Circuits Syst. II. Express Briefs* **2020**, *10*, 67. [CrossRef]

38. Khatibi, M.; Haeri, M. Fault-Tolerant Control for Linear Time-Variant Impulsive Singular Systems Subject to Actuator Saturation and L-infinity Disturbances. *J. Dyn. Syst. Meas. Control* **2017**, *11*, 139.

39. Zhou, B. Analysis and design of discrete-time linear systems with nested actuator saturations. *Syst. Control. Lett.* **2013**, *62*, 871879. [CrossRef]

40. Chen, Y.; Wang, Z.; Fei, S.; Han, Q. Regional stabilization for discrete time-delay systems with actuator saturations via a delay-dependent polytopic approach. *IEEE Trans. Autom. Control* **2018**, *64*, 1257–1264. [CrossRef]

41. Banu, L.J.; Balasubramaniam, P.; Ratnavelu, K. Robust stability analysis for discrete-time uncertain neural networks with leakage time-varying delay. *Neurocomputing* **2015**, *151*, 808–816. [CrossRef]

42. Seuret, A.; Gouaisbaut, F. Wirtinger-based integral inequality: Application to time-delay systems. *Automatica* **2013**, *49*, 2860–2866. [CrossRef]

43. Tarbouriech, S.; Prieur, C.; Silva, J. Stability analysis and stabilization of systems presenting nested saturations. *IEEE Trans. Autom. Control* **2006**, *51*, 1364–1371. [CrossRef]